Integration of Point Cloud Data for Numerical Simulations Using NURBS Surfaces

Andreas-Nizar Granitzer
Institute of Soil Mechanics, Foundation Engineering and Computational Geotechnics, Graz University of Technology, Graz, Austria

Franz Tschuchnigg
Institute of Soil Mechanics, Foundation Engineering and Computational Geotechnics, Graz University of Technology, Graz, Austria

Wolfgang Summerer
Geotechnical Department, ILF Consulting Engineers Austria GmbH, Rum, Austria

ABSTRACT: The numerical modelling of complex surface geometries represents a challenging task in computational geotechnics. Corresponding problem classes include non-horizontal topographic surfaces (TS) in mountainous terrain, rock mass discontinuities or steep slopes, presumably inducing significant stress redistributions in the project domain that need to be considered. This raises an obvious question at the interface with geographic information systems: How to integrate point-based surveying measurements defining the TS into the numerical modelling process? In this respect, we present a step-by-step methodology based on survey data from two infrastructure projects in Austria, at the core of which NURBS surfaces are used to generate TS models with high accuracy.

Keywords: NURBS, GIS-to-FEM, point pattern analysis, optimal tunnel route, topographic surface.

1 INTRODUCTION

The growing advancement of hardware and software technologies has paved the way to large-scale three-dimensional (3D) finite element analyses (FEA), allowing for the consideration of large topographic surfaces (TS) in combination with reasonably fine finite element mesh resolutions. In this respect, powerful features that deserve attention include but not limited to advanced preconditioning strategies to efficiently approximate the solution to boundary value problems (Chaudhary et al. 2013) and drone-enabled topographical surveying methods, such as photogrammetry or LiDAR (light detection and ranging).

The set of 3D spatial point vectors $\boldsymbol{x} \in \mathbb{R}^3$ obtained from the latter can subsequently be integrated into the finite element modelling process (FEMP) by employing spatial interpolation techniques, shifting the emphasis of analyses from analytical or empirical approaches to large-scale 3D FEA; typical civil engineering problems where large-scale simulations are proving increasingly beneficial comprise multi-temporal analyses of open-pit mines (Jerman et al. 2021), remediation designs for powerhouse caverns (Tschuchnigg und Dich 2020), ground pressure estimations required for the dimensioning of pressure shafts (Innerhofer und Greiner 2019) or the determination of alarm values during the construction of underground railway passages (Granitzer et al. 2021).

As a scientific contribution to this work, we propose a NURBS surface-based procedure for integrating terrestrial 3D point cloud vector data (NPTP) into the FEMP. The paper is therefore structured as follows: Section 2 gives an overview of the theoretical framework with respect to the NPTP on the basis of synthetic demonstration cases, using point cloud (PC) data from an ongoing railway construction project in Austria (Seywald und Rettenbacher 2022). In section 3, we present a case study in which the NPTP has been employed to perform FEA in course of the pumped-storage hydropower plant project Lünerseewerk II, Austria. Section 4 highlights the main conclusions.

2 BACKGROUND

2.1 Spatial point pattern analysis

Within the scope of envisaged application classes, $\boldsymbol{x}$ are sampled along equally spaced parallel lines, i.e., elevations in the z-direction are measured over a squared planar grid defined above a horizontal (x,y) plane; see **Figure 1 (a)**. The accuracy of TS generated from so-called grid PC is considerably governed by the point cloud density (PCD) describing the spatial variation of $\boldsymbol{x}$ in the observation window (Agüera-Vega et al. 2020); traditionally, more accurate approximations of the actual TS are achieved with higher PCD. From a numerical point of view, however, a higher PCD implies longer processing times during both the spatial interpolation as well as FEA and is more prone to obstacles arising in the domain discretization. In many cases, it is therefore reasonable to adaptively decrease the PCD in areas in which only a moderate resolution of the TS is required while keeping the PCD in selected areas at high levels. For example, this may be stipulated in areas that show steep gradients; hence, an accurate geometrical representation of the TS is in demand to recover a realistic stress state from FEA. This concern motivates a point cloud modification process (PCMP), after which PCs remain no longer systematic in nature, but show an adaptive spatial point pattern; cf. Bolstad (2019).

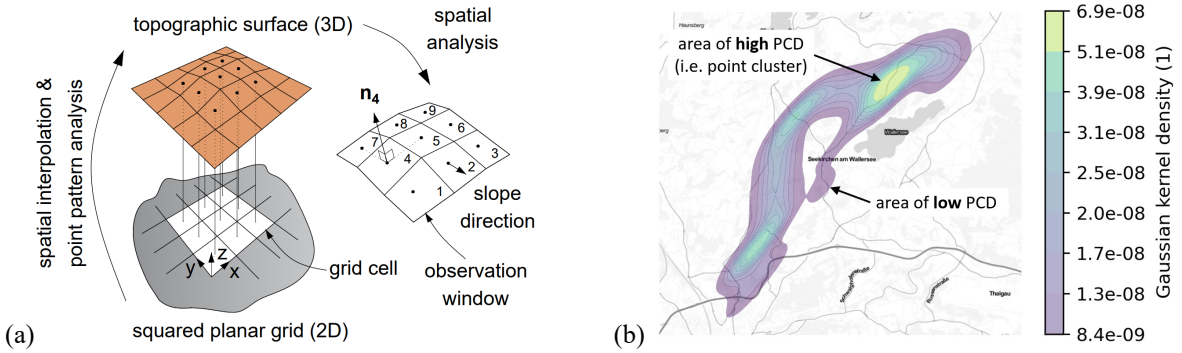

Figure 1. (a) Topographic surface-from-point generation procedure; (b) density-based point pattern analysis employing the bi-variate Gaussian density estimation method, i.e., the integral over the study area is 1.

To strike a balance between acceptable computational expense and adequate geometrical representation of the TS in large-scale FEA, density-based point pattern analyses (db-PPA) offer attractive features to control the PCMP by providing detailed insight to the distribution of $\boldsymbol{x}$ in terms of PCD (Boots und Getis 1988). It should be noted, however, that db-PPA are prone to the modifiable areal unit problem (MAUP), first discussed by Openshaw (1984), i.e., the results may significantly vary depending on the shape, size and position of aggregation units considered in the grouping of $\boldsymbol{x}$. Continuous db-PPA methods, such as the bi-variate Gaussian spatial kernel density estimation (KDE) exemplified in **Figure 1 (b)**, represent attractive methods to work around the MAUP. The basic idea of KDE is to count the number of $\boldsymbol{x}$ at the position of interest in a continuous way, using kernels that assign distance-based weights to all $\boldsymbol{x}$ considering a moving sub-region window. As a side note, KDE should not be confused with discrete db-PPA, such as hexagonal binning (Brunsdon und Comber 2019), in which $\boldsymbol{x}$ are equally counted in case they are located inside boundaries of non-overlapping aggregation units. Interested readers may refer to MacLachlan (2022) and Gramacki (2018) for more details on the background of db-PPA and kernel mapping methods, respectively.

2.2 *Spatial interpolation techniques*

In addition to the spatial distribution of $\boldsymbol{x}$, the spatial interpolation technique (SIT) employed to form a surface out of (discrete) $\boldsymbol{x}$ may yield crucial to achieve an accurate geometrical TS representation at unsampled locations $\boldsymbol{x_u}$ (Englund 1990). This conversion process described by **Figure 1 (a)**, also known as contouring or surface modelling (Yang und Hodler 2000), can be realized by a variety of SIT types; available approaches range from deterministic techniques based on either the smoothing degree (e.g., radial basis function) or the extent of similarity (e.g., inverse distance weighting) to geostatistical techniques, such as kriging, which additionally account for the spatial configuration of sampled $\boldsymbol{x}$ around prediction locations. In view of the quality of the interpolated elevation estimates at $\boldsymbol{x_u}$, numerous publications (Agüera-Vega et al. 2020) report that the optimal SIT is problem-dependent; hence, the suitability of SIT has to be assessed on a case-by-case basis; cf. **Figure 2 (a)**.

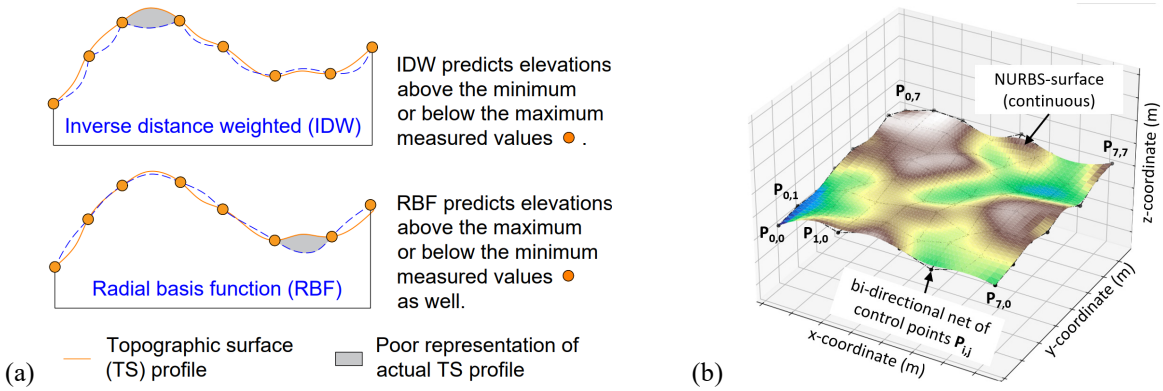

Figure 2. (a) Comparison of deterministic spatial interpolation techniques (inverse distance weighting versus radial basis function) and (b) example of bi-cubic NURBS surface, i.e., $p = q = 3$.

Regarding geotechnical FEA, the most commonly used surface modelling approach is perhaps the triangular irregular network (TIN) model, in which elevations at $\boldsymbol{x_u}$ are approximated by contiguous non-overlapping triangular facets of irregular shape and size (Lee 1991). The high potential of TINs for modelling TS is mainly attributed to their ability to accommodate irregularly spaced $\boldsymbol{x}$ and their efficiency in data storage of heterogeneous TS (Lim und Pilesjö 2022). However, as a consequence of the PCMP followed in this work, the triangulation procedure associated with TIN may trigger numerical problems caused by triangles of different size, in particular by skinny and long distorted triangles (Piegl und Tiller 1995). As will be described in **Section 2.3**, NURBS surfaces may serve as powerful alternatives to circumvent these limitations on the one hand, while allowing for a reasonably accurate representation of the TS in areas with steep gradients on the other hand.

2.3 *NURBS surface fundamentals*

Over the last decade, NURBS surfaces have found wide application in computational geotechnics; for example, Coombs et al. (2016) have applied this concept to define the yield surface within the framework of NURBS plasticity, while Ma et al. (2022) have incorporated NURBS surfaces to detect critical slip surfaces in slope stability analyses. From a mathematical point of view, NURBS (non-uniform rational B-spline) surfaces represent bi-variate vector-valued piecewise rational functions, with which the elevation at a given parametric position ($u, v \in [0,1]$) is defined by **Equation (1)**:

$$\boldsymbol{S}(u,v) = \sum_{i=0}^{n} \sum_{j=0}^{m} R_{i,j}(u,v) \cdot \boldsymbol{P_{i,j}} \tag{1}$$

where $\{\boldsymbol{P_{i,j}}\}$ forms a bi-directional net composed of an $n \times m$ array of control points $\boldsymbol{P_{i,j}}$, displayed by **Figure 2 (b)**. Piecewise rational basis functions $R_{i,j}$ belonging to $\boldsymbol{P_{i,j}}$ are given by **Equation (2)**:

$$R_{i,j}(u,v) = \frac{N_{i,p}(u) \cdot N_{j,q}(v) \cdot w_{i,j}}{\sum_{k=0}^{n} \sum_{l=0}^{m} N_{k,p}(u) \cdot N_{l,q}(v) \cdot w_{k,l}} \quad (2)$$

where $N_{i,p}$ and $N_{i,q}$ are the non-rational B-spline basis functions of degrees p (in u-direction) and q (in v-direction), and $\{w_{i,j}\}$ are the weights associated with $\boldsymbol{P_{i,j}}$. The denominator accounts for the partition of unity property, i.e., $\sum_{i=0}^{n} \sum_{j=0}^{m} R_{i,j}(u,v) = 1, \forall\, (u,v) \in\ [0,1] \times [0,1]$. In the scope of this work, the weights at $\boldsymbol{P_{i,j}}$ are defined uniform, whereas NURBS surface knot vectors are clamped, i.e., the corner positions of the NURBS surface coincide with the control point net; cf. **Figure 2 (b)**. More detailed information regarding NURBS surfaces can be found in Piegl and Tiller (1995).

3 CASE STUDY

3.1 Project description and analysis aim

Preliminary 3D FEA have been carried out as a supplemental basis for the decision-making about the optimal routes of the P-SHP network Lünerseewerk II located in Vorarlberg, Austria. At this point, the numerical studies have focused on the analysis of principal stress (PS) distributions computed for different variant cases, a key aspect in the structural design of underground structures forming P-SHP (Seeber 1999). As illustrated in **Figure 3 (a)**, the TS of the analysis domain ($x \times y = 10 \times 18\ km$) is characterized by a high level of spatial variability ($z \in [517, 2950]\ m$), resulting in considerable principal stress rotations induced by arching effects, particularly at shallow depths; consequently, the suitability of simplified analytical or empirical relationships between the overburden height and principal stresses is far from warranted, i.e., in extreme cases their application may cause severe damages (Innerhofer und Greiner 2019). To achieve more reliable PS predictions, we propose a practical NPTP which allows for efficient integration of point-based TS surveying measurements into FEA, as will be further discussed below.

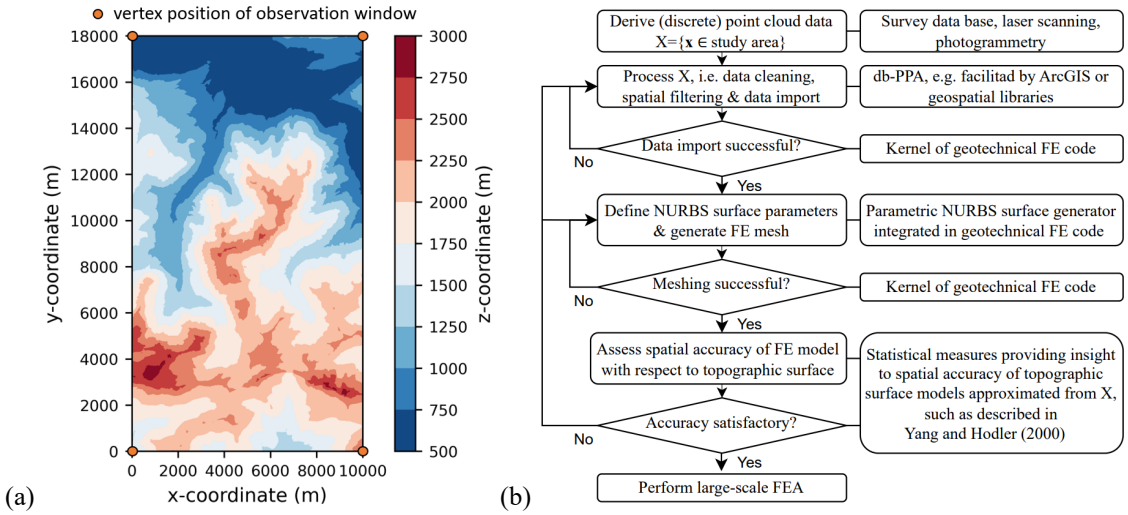

Figure 3. (a) TS presented in TIN data model; (b) NURBS surface-based FE model development.

3.2 NURBS-based finite element model development

Figure 3 (b) provides a detailed flowchart of the proposed NPTP, including (rectangular-framed) activities and (diamond-framed) decision boxes described in the left column, as well as related facilitation tools reported in the right column. For brevity, only selected aspects can be highlighted:

- The NPTP is promoted by FE codes with integrated parametric NURBS surface functionality, such as Plaxis 3D (Bentley Systems 2021). In this way, related parameters

described in **Section 2.3** can be defined without the need for an interim step where NURBS surfaces have to be built by third-party tools (e.g., Jerman et al. 2021).

- Two governing factors controlling the spatial accuracy of the TS model (Yang und Hodler 2000) have been identified, namely the number of control points and (local) PCD; see also **Figure 1 (b)** and **Figure 2 (b)**. To satisfy TS model accuracy criterions, it is therefore recommended to iteratively increase one of these factors, particularly in hilly areas.
- To avoid discretization errors, the point cloud data set X used as basis for NURBS surface modelling should include $\boldsymbol{x}$ located at the observation window vertices; cf. **Figure 3 (a)**.

3.3 Preliminary finite element investigations

Figure 4 (a) displays the discretized domain, at the top of which we have deployed the NPTP to generate the TS model. In the present case, X (i.e., consisting of around 150.000 $\boldsymbol{x}$) is obtained from both surveying measurements and existing survey data bases, defined in two different terrestrial reference systems; hence, the integration of $\boldsymbol{x}$ into one local reference system required the application of geospatial libraries. To increase the accuracy of the TS model, the PCD is locally increased towards critical areas applying db-PPA; cf. **Section 2.1**. Moreover, the control point net is iteratively densified, resulting in around 72.000 control points. The standard deviation of the difference between the measured and interpolated z-coordinates obtained at all $\boldsymbol{x}$ withheld in the observation window is approximately 8 meters, which has been considered sufficient at this early stage in the planning.

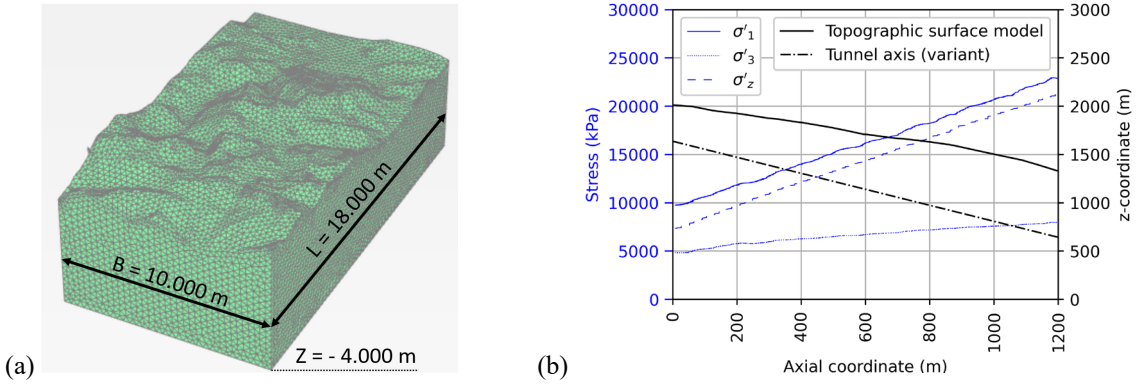

Figure 4. (a) NURBS surface-enabled mesh; (b) primary (principal) stress distribution along tunnel section.

Figure 4 (b) provides insight into the distribution of PS and vertical stresses σ'_z computed along an exemplary tunnel axis located below a steep slope. It becomes evident that the results are significantly influenced by stress redistributions and principal stress rotations triggered by the rapidly varying TS model. It should be noted that parametric FEA have been carried out considering an elasto-plastic constitutive model with non-associated flow rule and a realistic bandwidth of constitutive parameters provided by the client. Future investigations are planned to be executed using site-specific ground investigation data, presumably involving rock mass discontinuities described by NURBS surfaces in combination with more advanced constitutive models.

4 CONCLUSIONS

The present work concerns the integration of point-based surveying data describing the topographic surface into the finite element modelling of large-scale domains. The proposed methodology employs NURBS surfaces to reduce irrelevant details in the point-to-surface conversion. Relevant aspects are discussed on the basis of two projects planned in Austria, including valuable tools that allow for a systematic increase in model accuracy. It is demonstrated that the geometrical representation of topographic surfaces may play a key role in numerical predictions addressing mountainous terrain. Future research effort should focus on the modelling of multiple NURBS surfaces, for example, in the context of rock mass discontinuities of BIM-to-FEM problems (e.g., Giangiulio et al. 2022).

ACKNOWLEDGEMENTS

The authors would like to express their gratitude to illwerke vwk AG and ILF Consulting Engineers Austria GmbH for giving the permission to publish project-related data.

REFERENCES

Agüera-Vega, F.; Agüera-Puntas, M.; Martínez-Carricondo, P.; Mancini, F.; Carvajal, F. (2020): Effects of point cloud density, interpolation method and grid size on derived Digital Terrain Model accuracy at micro topography level. In: International Journal of Remote Sensing 41 (21), S. 8281–8299.

Bentley Systems (2021): Scientific Manual. Plaxis Connect Edition V22.00.

Bolstad, Paul (2019): GIS Fundamentals: a first text on geographic information systems. A first text on geographic information systems. 6th ed. Ann Arbor, MI: Paul Bolstad.

Boots, B. N.; Getis, Arthur (1988): Point pattern analysis. Newbury Park, Calif.: Sage Publications.

Brunsdon, Chris; Comber, Lex (2019): An introduction to R for spatial analysis & mapping. Second edition. London, Thousand Oaks CA, New Delhi, Singapore: SAGE (Spatial analytics and GIS).

Chaudhary, K. B.; Phoon, K. K.; Toh, K. C. (2013): Effective block diagonal preconditioners for Biot's consolidation equations in piled-raft foundations. In: Int. J. Numer. Anal. Meth. Geo. (International Journal for Numerical and Analytical Methods in Geomechanics) 37 (8), S. 871–892.

Coombs, William M.; Petit, Oscar A.; Ghaffari Motlagh, Yousef (2016): NURBS plasticity: Yield surface representation and implicit stress integration for isotropic inelasticity. In: Computer Methods in Applied Mechanics and Engineering 304, S. 342–358. DOI: 10.1016/j.cma.2016.02.025.

Englund, Evan J. (1990): A variance of geostatisticians. In: Math Geol 22 (4), S. 417–455.

Giangiulio, Michael; Granitzer, Andreas-Nizar; Tschuchnigg, Franz; Hoffmann, Jens (2022): BIM-to-FEM: Development of a Software Tool to Increase the Operational Efficiency of Dam Construction Projects. In: António Gomes Correia, Miguel Azenha, Paulo J. S. Cruz, Paulo Novais und Paulo Pereira (Hg.): Trends on construction in the digital era. Proceedings of isic 2022, Bd. 306: Springer int. PU, S. 182–195.

Gramacki, Artur (2018): Nonparametric Kernel Density Estimation and Its Computational Aspects. 1st edition 2018. Cham: Springer International Publishing (Studies in Big Data, 37).

Granitzer, Andreas; Tschuchnigg, Franz; Summerer, Wolfgang; Galler, Robert; Stoxreiter, Thomas (2021): Construction of a railway tunnel above the main drainage tunnel of Stuttgart using the cut-and-cover method. In: Bauingenieur 96 (05), S. 156–164. DOI: 10.37544/0005-6650-2021-05-40.

Innerhofer, Guntram; Greiner, Richard (2019): Structural design concept for pressure shafts of hydro plants using the passive resistance of the rock mass. In: Geomechanics and Tunnelling 12 (3), S. 270–281.

Jerman, J.; Sayed, M. El; Mašín, D.; Kadlíček, T. (2021): A Procedure for 3D Modelling of Very Large Geotechnical Structures: Open Cast Coal Mine Case. In: Marco Barla, Alice Di Donna und Donatella Sterpi (Hg.): Challenges and Innovations in Geomechanics, Bd. 126: Springer int. PU, S. 36–43.

Lee, Jay (1991): Comparison of existing methods for building triangular irregular network, models of terrain from grid digital elevation models. In: Int. journal of geographical information systems 5 (3), S. 267–285.

Lim, Jana; Pilesjö, Petter (2022): Triangular Irregular Network (TIN) Models. In: GIS&T BoK 2022 (Q2).

Ma, Terence; Mafi, Ramin; Cami, Brigid; Javankhoshdel, Sina; Gandomi, Amir H. (2022): NURBS Surface-Altering Optimization for Identifying Critical Slip Surfaces in 3D Slopes. In: Int. J. Geomech. 22 (9).

MacLachlan, Andrew; Dennett, Adam (2022): An Applied Geographic Information Systems and Science Course in R. In: JOSE 5 (50), S. 141. DOI: 10.21105/jose.00141.

Openshaw, Stan (1984): The modifiable areal unit problem. Norwich: Geo Abstracts Univ. of East Anglia.

Piegl, Leslie A.; Tiller, Wayne (1995): The NURBS Book. Berlin, Heidelberg: Springer Berlin Heidelberg.

Seeber, Gerhard (1999): Druckstollen und Druckschächte. Bemessung - Konstruktion Ausführung. Stuttgart: Enke im Thieme Vlg.

Seywald, Christian; Rettenbacher, Martin (2022): The new railway line between Köstendorf and Salzburg – Looking back to the past and forward to the future. In: Geomechanics and Tunnelling 15 (6), S. 711–719.

Tschuchnigg, F.; Dich, C. (2020): Powerhouse cavern Obervermuntwerk II – Analysis and remediation of the shotcrete spalling. In: Bauingenieur 95 (12), S. 473–480. DOI: 10.37544/0005-6650-2020-12-39.

Yang, Xiaojun; Hodler, Thomas (2000): Visual and Statistical Comparisons of Surface Modeling Techniques for Point-based Environmental Data. In: Cartography and Geographic Information Sc. 27 (2), S. 165–176.